CDF note 10160

Measurement of the Cross Section for Prompt Isolated Diphoton Production with 9.5 fb^{-1} of CDF Run II Data

The CDF Collaboration
URL http://www-cdf.fnal.gov
(Dated: June 7, 2012)

A measurement is reported of the cross section of prompt isolated photon pair production in $p\overline{p}$ collisions at a total energy $\sqrt{s} = 1.96$ TeV using data of 9.5 fb^{-1} integrated luminosity collected with the CDF II detector at the Fermilab Tevatron. The measured differential cross section is compared with six perturbative QCD predictions, a Leading Order (LO) parton shower Monte Carlo, four Next-to-Leading Order (NLO) calculations, and one NNLO calculation. The NLO and NNLO calculations reproduce most aspects of the data. By including photon radiation from quarks before and after hard scattering, the parton shower Monte Carlo becomes competitive with the NLO and NNLO predictions.

Preliminary Results for Summer 2012 Conferences

I. INTRODUCTION

The production of prompt photon pairs with large invariant mass in hadron collisions is a large irreducible background in searches for a low mass Higgs boson decaying into a photon pair [1], as well as in searches for new phenomena, such as new heavy resonances [2], extra spatial dimensions [3, 4] or cascade decays of heavy new particles [5]. Precise measurements of the diphoton production differential cross sections for various kinematic variables and their theoretical understanding are thus very important for these searches. Diphoton production is also used to check the validity of perturbative quantum chromodynamics (pQCD) and soft-gluon resummation methods implemented in theoretical calculations. Diphotons are expected to be dominantly produced by quark-antiquark annihilation $q\overline{q} \to \gamma\gamma$ and in kinematic regions with high gluon luminosity, especially at low invariant mass, by gluon-gluon fusion $gg \to \gamma\gamma$ through a quark loop diagram. Prompt photons may also result from quark fragmentations in the hard scattering, although a strict photon isolation requirement significantly reduces the fragmentation contributions.

Diphoton measurements have been previously conducted at fixed-target [6] and collider experiments [7–10]. The most recent measurements [9, 10] were compared with the same pQCD calculations examined in the present work and large discrepancies were found between the data and a parton shower Monte Carlo (MC), suitable for simulation of the backgrounds in searches of a low mass Higgs boson and of new phenomena. This work shows that the inclusion of photons radiated from initial and final state quarks drastically improves the comparison of the parton shower calculation with the data. This note is an update of the CDF published result using 5.36 fb^{-1}.

II. DATA SAMPLE & EVENT SELECTION

This analysis is based on data collected with the CDF IIb detector between February 2002 and September 2011, the complete Run II dataset. The integrated luminosity for all good runs of this time period is 9.5 fb^{-1}. The data are collected with a diphoton trigger requiring two EM clusters, each of $\mathrm{E_T} > 12$ GeV, with CES $\chi^2 < 20$ and fiducial to the CEM calorimeter, which implies a range of $|y| \leq 1$ in the rapidity of each photon. Two main cuts are applied: (i) On the transverse energy $E_T \geq 17$ GeV for the first photon in the event and $E_T \geq 15$ GeV for the second photon; (ii) on the calorimeter isolation energy of each photon to be at most 2 GeV with a very mild increase of this cutoff with increasing photon E_T. The isolation cone is defined so as to have a radius $R = \sqrt{(\Delta\eta)^2 + (\Delta\phi)^2} = 0.4$ around the axis of the shower profile in the space of the photon pseudo-rapidity η and azimuth ϕ with reference to the detector coordinate system. The isolation cut implies that the angular separation of the two photons in the event is $\Delta R \geq 0.4$.

III. BACKGROUND SUBTRACTION

The sample selected as described in the previous section is still a compound of photons coming directly from the colliding hadrons ("prompt" photons) and of photons created within jets of hadrons which are copiously produced from high energy colliding beams. The signal for the diphoton cross section measurement is the sub-sample of prompt photons. The background of non-prompt photons is subtracted from the total sample with a method based on the photon isolation. In this measurement the track isolation is used, defined as the scalar sum of the transverse momenta of all tracks originating from the primary vertex of the event and lying within the photon isolation cone. In contrast with the calorimeter isolation, the track isolation does not depend (i) on the multiple interactions between different pairs of colliding hadrons, due to the primary vertex requirement, and (ii) on the energy leakage from the calorimeter cluster. It can thus be used to separate signal and background photons with less systematic uncertainty.

The background is subtracted with a statistical procedure by testing each photon for whether or not its track isolation is lower (signal-like) or higher (background-like) than a cutoff. The cutoff detemined to 1 GeV/c by optimizing the signal and background efficiencies for passing the track isolation cut for maximum separation between signal and background. The weights are used in a 4×4 matrix equation which is solved for the probabilities of pure signal, pure background and mixed photon pairs with input the weights for all four possible combinations of the leading or sub-leading photon passing or failing the track isolation cut. These probabilities are functions of the efficiencies of signal and background photons for passing the cut, which in turn are functions of the photon E_T. The efficiencies are determined from Monte Carlo photon+jet samples, for the signal, and dijet samples, for the background, produced using the Pythia event generator [11], with the events fully simulated through the detector using the Geant program and reconstructed using the CDF IIb reconstruction software [12]. In this way the full correlations between the two photons in each event are properly taken into account. The systematic uncertainty in the signal fraction achieved with the track isolation method is of the order of 15-20%, as shown in Figure 1. The method is tested by measuring a fraction consistent with 100% in a signal Monte Carlo sample and consistent with 0% purity in a background Monte Carlo sample.

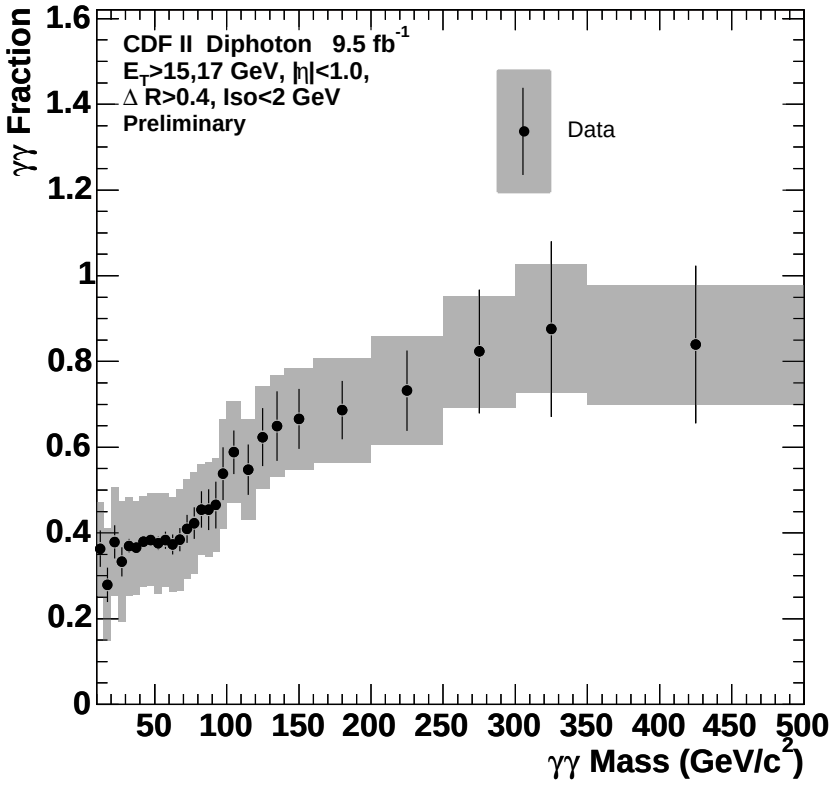

FIG. 1: Estimated signal fraction as a function of the diphoton mass.

IV. CORRECTIONS AND NORMALIZATION

The diphoton production cross section differential in a kinematic variable, averaged over a bin of the variable, is determined by dividing the number of signal events in the bin by the trigger efficiency, the diphoton selection efficiency, the integrated luminosity and the bin size. The diphoton trigger efficiency is derived from data. It is consistent with 100% over all of the kinematic range with a flat uncertainty of 3%. The selection efficiency is determined from data and Monte Carlo with an iterative method. In the first pass the efficiency is determined from a fully simulated and reconstructed Pythia diphoton Monte Carlo sample by dividing the number of events passing all selection cuts by the number of events passing only the kinematic cuts on the photon E_T, η, angular separation and event generator isolation. The estimated signal events of the data are corrected for this preliminary selection efficiency. They are also corrected for the "underlying event" from gluon radiation and spectator quark activity which make the efficiency derived from Pythia too high by removing events from the denominator through the isolation cut. This correction is derived from Monte Carlo with and without underlying events and amounts to a constant factor of 0.88 per event. The data are then used to reweigh the Pythia events and obtain a better representation of the true diphoton distribution. The efficiency is determined again using the reweighted Pythia sample and finally corrected for a luminosity dependence, derived from comparison of the number of vertices distributions in data and Pythia Monte Carlo $Z^0 \to e^+e^-$ events. The uncertainty in the selection efficiency, coming from the luminosity dependence correction, grows linearly from 1.8% for $E_T \leq 40$ GeV to 3% at $E_T = 80$ GeV and remains constant above this point. A flat 6% uncertainty (3% per photon) comes from the underlying event correction. Finally, a 6% constant uncertainty comes from the Tevatron integrated luminosity.

The $Z^0 \to e^+e^-$ sample is used for calibration by applying "diphoton-like" event selection, i.e. imposing diphoton selection but allowing for a track associated with each one of the two prompt electromagnetic objects in the event. The electromagnetic energy scale in data and Monte Carlo is corrected by tuning the $Z^0 \to e^+e^-$ mass peak to the world average [13] and an uncertainty from this correction is estimated to grow linearly from 0 at $E_T \leq 40$ GeV up to 1.5% at $E_T = 80$ GeV and remain constant above this point. All systematic uncertainties in the cross section

measurement are added in quadrature. As a final cross check the $Z^0 \to e^+e^-$ cross section is measured in the range between 65 and 115 GeV/c^2 of the e^+e^- mass using the diphoton-like event selection and all of the corrections and normalizations applied to the diphoton cross section. The result of (256 ± 3) pb^{-1} is in good agreement with the known value of 254 pb^{-1} [14].

V. CALCULATIONS COMPARED WITH THE DATA

The results of this measurement are compared with six theoretical calculations: (i) the predictions of the PYTHIA program [11] which features a realistic representation of the physics events by including parton showering, Initial (ISR) and Final State Radiation (FSR) and an underlying event model (ii) the fixed NLO predictions of the DIPHOX program [15] including parton fragmentations into photons [16], (iii) the predictions of the RESBOS program [17] where the cross section is accurate to NLO, but also has an analytical initial state soft gluon resummation, (iv) the NLO prediction of the **MCFM** program [18] with non-perturbative contributions to fragmentation (v) the prediction of **SHERPA** [19] where the NLO production is passed to a novel program for modeling the transition to non-perturbative showering and (vi) the prediction of a recent fixed–order NNLO calculation [20].

To create the PYTHIA model, diphoton events were filtered from an inclusive γ+X PYTHIA sample (X=γ or jet), thus including the $q\bar{q} \to \gamma\gamma$ and $gg \to \gamma\gamma$ processes (56%) as well as the $q\bar{q} \to g\gamma\gamma_{\rm ISR}$, $gq \to q\gamma\gamma_{\rm ISR}$ and $gq \to q\gamma\gamma_{\rm FSR}$ processes (44%). This type of calculation effectively resums the cross section for gluon and photon radiation both in the initial and the final state.

All calculations are subject to the experimental kinematic and isolation cuts. DIPHOX accounts for the $gg \to \gamma\gamma$ process in LO only. The predictions of RESBOS are restricted in the invariant mass range from $2m_b = 9$ GeV/c^2 to $2m_t = 350$ GeV/c^2, where m_b and m_t are the masses of the bottom and top quarks, respectively. NLO theoretical uncertainties are estimated by varying the renormalization, factorization and fragmentation (in DIPHOX only) scales up and down by a factor of 2 relative to the default scale $\mu = M/2$ of DIPHOX and $\mu = M$ of RESBOS, and for the NLO PDF uncertainties (in both DIPHOX, RESBOS, and MCFM) by using the 20 CTEQ6.1M eigenvectors. Uncertainties in the **MCFM** and NNLO predictions were provided by the authors of those models. [21].

VI. RESULTS

Figure2 2 and 3 show the comparison between the measured and predicted diphoton distributions: the diphoton invariant mass M, the diphoton transverse momentum $P_{\rm T}$ and the difference $\Delta\phi$ between the azimuthal angles of the two photons in the event. While the PYTHIA direct calculation ($\gamma\gamma$) fails to describe both the scale and shape of the data, including radiation brings the prediction in fair agreement with the data. The mass distributions show a reasonable agreement with the data for all predictions above the peak at 30 GeV/c^2, particularly in the region 80 GeV/c^2 $< M <$ 150 GeV/c^2 relevant to searches for the Higgs boson [1]. (The RESBOS and NNLO tend to be about 20However, all predictions underestimate the data around and below the peak, but the NNLO prediction is notably better than the rest.

In the $P_{\rm T}$ spectrum all predictions except SHERPA and NNLO underestimate the data in the region between 20 and 50 GeV/c. For $P_{\rm T}<20$ GeV/c, where soft gluon resummation is most important, only the RESBOS and SHERPA predictions describe the data.

Discrepancies between data and theory are most prominent in the comparison of the measured and predicted distributions of $\Delta\phi$. In this case all predictions except NNLO fail to describe the data across the whole spectrum. Approaching $\Delta\phi = \pi$, where soft gluon processes are expected to manifest, the RESBOS and SHERPA predictions tend to agree better with the data. In the range 1.4 rad$<\Delta\phi<$2.2 rad the PYTHIA and SHERPA predictions describe the data. In the low $\Delta\phi$ tail, which corresponds to the region of low M ($<$50 GeV/c^2), all predictions except NNLO are lower than the data.

In total, the NNLO and SHERPA predictions tend to predict the data most accurately, though neither is completely free of descrepancies, and measurement systematics are non-negligible.

VII. SUMMARY

In summary, the diphoton production cross section, differential in kinematic variables sensitive to the reaction mechanism, is measured using 9.5 fb^{-1} of data collected with the CDF II detector. The high statistics of the measured sample allows for a higher precision scan over a much more extended phase space than previous measurements. The

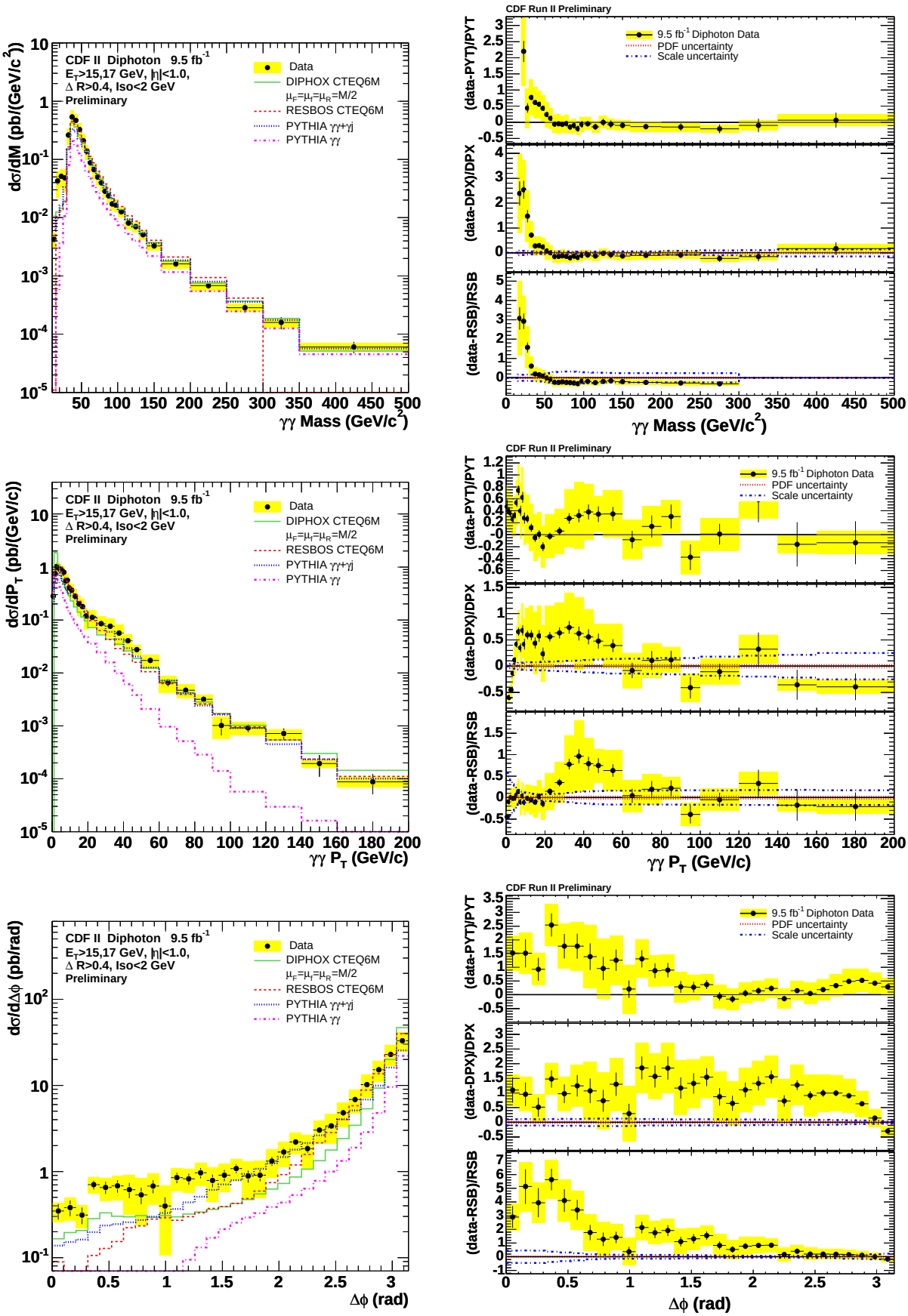

FIG. 2: **Top:** The measured differential cross section compared with the first three theoretical models discussed in the text. **Left** windows show the absolute comparison and **right** windows show the fractional deviations of the data points from the model predictions. The comparisons are made as functions of the diphoton mass (**top**), transverse momdentum (**middle**) and azimuthal difference (**bottom**). The shaded area around the data points shows the total systematic uncertainty of the measurement.

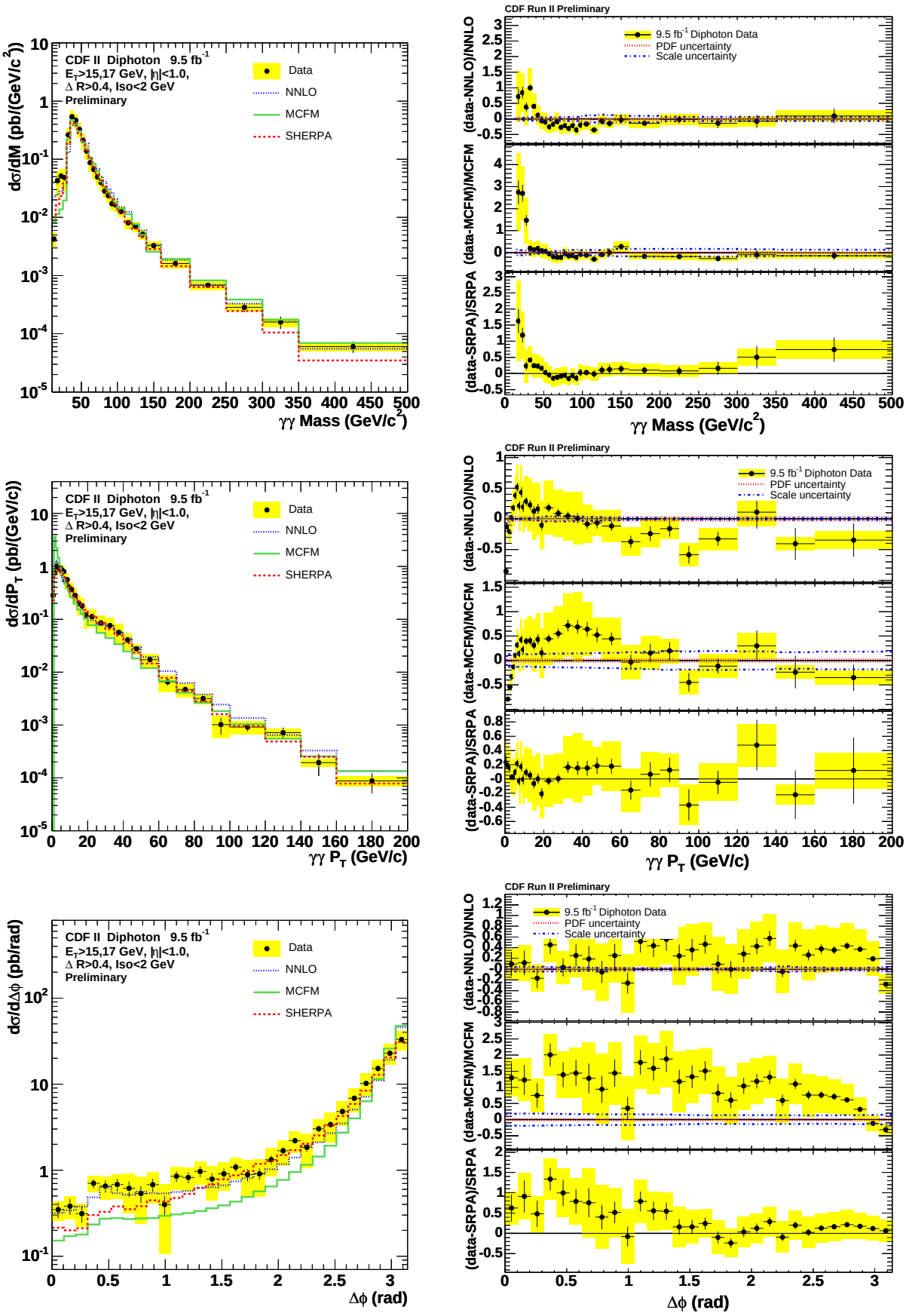

FIG. 3: **Top:** The measured differential cross section compared with the second three of the six theoretical models discussed in the text. **Left** windows show the absolute comparison and **right** windows show the fractional deviations of the data points from the model predictions. The comparisons are made as functions of the diphoton mass (**top**), transverse momdentum (**middle**) and azimuthal difference (**bottom**). The shaded area around the data points shows the total systematic uncertainty of the measurement.

overall systematic uncertainty is limited to about 30%. The results of the measurement are compared with state-of-the-art caclulations, applying complementary techniques in describing the reaction. All NLO and NNLO calculations, within their known limitations, reproduce the main features of the data. By including photon radiation in the initial and final states, a parton shower MC suitable for background simulations in searches for a low mass Higgs boson and new phenomena describes the data, within uncertainties, in most kinematic regions.

Acknowledgments

We thank the Fermilab staff and the technical staffs of the participating institutions for their vital contributions. We also thank P. Nadolsky, C.-P. Yuan, Z. Li, J.-P. Guillet, C. Schmidt and S. Mrenna for their valuable help in the theoretical calculations. This work was supported by the U.S. Department of Energy and National Science Foundation; the Italian Istituto Nazionale di Fisica Nucleare; the Ministry of Education, Culture, Sports, Science and Technology of Japan; the Natural Sciences and Engineering Research Council of Canada; the National Science Council of the Republic of China; the Swiss National Science Foundation; the A.P. Sloan Foundation; the Bundesministerium für Bildung und Forschung, Germany; the World Class University Program, the National Research Foundation of Korea; the Science and Technology Facilities Council and the Royal Society, UK; the Institut National de Physique Nucleaire et Physique des Particules/CNRS; the Russian Foundation for Basic Research; the Ministerio de Ciencia e Innovación, and Programa Consolider-Ingenio 2010, Spain; the Slovak R&D Agency; and the Academy of Finland.

[1] T. Aaltonen *et al* (CDF Collaboration), Phys. Rev. Lett. **103**, 061803 (2009); V. M. Abazov *et al* (D0 Collaboration), Phys. Rev. Lett. **102**, 231801 (2009); G. And *et al* (ATLAS Collaboration), arXiv:0901.0512 [hep-ex] (2009); G. L. Bayatian *et al* (CMS Collaboration), J. Phys. G **34**, 995 (2007).
[2] S. Mrenna and J. Willis, Phys. Rev. D **63**, 015006 (2001), and references therein.
[3] M. C. Kumar, P. Mathews, V. Ravindran and A. Tripathi, Phys. Lett. B **672**, 45 (2009).
[4] T. Aaltonen *et al*, Phys. Rev. Lett. **99**, 171801 (2007).
[5] G. F. Giudice and R. Rattazzi, Phys. Rep. **322**, 419 (1999).
[6] E. Bonvin *et al* (WA70 Collaboration), Z. Phys. C **41**, 591 (1989); Phys. Lett. B **236**, 523 (1990).
[7] C. Albajar *et al* (UA1 Collaboration), Phys. Lett. B **209**, 385 (1988).
[8] J. Alitti *et al* (UA2 Collaboration), Phys. Lett. B **288**, 385 (1992).
[9] F. Abe *et al* (CDF Collaboration), Phys. Rev. Lett. **70**, 2232 (1993); D. Acosta *et al* (CDF Collaboration), Phys. Rev. Lett. **95**, 022003 (2005), T. Aaltonen *et al.* (CDF Collaboration) Phys. Rev. **D**84, 052006 (2011), T. Aaltonen *et al.* (CDF Collaboration) Phys. Rev. Lett **107**, 102003 (2011).
[10] V. M. Abazov *et al* (D0 Collaboration), Phys. Lett. B **690**, 108 (2010).
[11] T. Sjostrand, P. Eden, C. Friberg, L. Lombard, G. Miu, S. Mrenna and E. Norrbin, Comp. Phys. Comm. **135**, 238 (2001); the version of Pythia used here is 6.2.16.
[12] E. Gerchtein and M. Paulini, CHEP-2003-TUMT005, arXiv:physics/0306031 (2003); the version of Geant used here is 3.21, see CERN Program Library Long Writeup W5013.
[13] W. M. Yao *et al*, "Review of Particle Physics", J. Phys. G **33**, 2006.
[14] D. Acosta *et al*, Phys. Rev. Lett. **94**, 091803 (2005).
[15] T. Binoth, J. P. Guillet, E. Pilon and M. Werlen, Eur. Phys. J. **C16**, 311 (2000); T. Binoth, J. P. Guillet, E. Pilon and M. Werlen, Phys. Rev. **D63**, 114016 (2001).
[16] L. Bourhis, M. Fontannaz and J. P. Guillet, Eur. Phys. J. **C2**, 529 (1998).
[17] C. Balazs, E. L. Berger, P. Nadolsky and C.-P. Yuan, Phys. Lett. **D637**, 235 (2006); C. Balazs, E. L. Berger, P. Nadolsky and C.-P. Yuan, Phys. Rev. **D76**, 013009 (2007); C. Balazs, E. L. Berger, P. Nadolsky and C.-P. Yuan, Phys. Rev. **D76**, 013008 (2007).
[18] J. M. Campbell *et al.*, Phys. Rev. **D**60 (1999) 113006.
[19] T. Gleisberg *et al.*, JHEP 02 (2009) 007.
[20] L. Cieri *et al.*, http://arxiv.org/abs/1110.2375 (2011).
[21] J. Pumplin, D. R. Stump, J. Huston, H. L. Lai, P. Nadolsky and W. K. Tung, J. HEP **0207**, 012 (2002).